CHAPTER 2

Integrated Computational and Experimental Approach for Novel Anti-Leishmanial Molecules by Targeting Dephospho-Coenzyme A Kinase

Abstract*

Coenzyme A acts as a necessary cofactor for many enzymes and is a part of many biochemical processes such as fatty acids, ketones and cholesterol metabolism. One of the critical enzymes involved in Coenzyme A synthesis is Dephospho-coenzyme A-kinase (DPCK). In this study, virtual screening and drug repurposing approaches have been employed to get a promising inhibitor of Dephospho-coenzyme A kinase using the natural products available in the ZINC database for anti-leishmanial drug development. The top hit compounds chosen after molecular docking were Veratramine, Azulene, Hupehenine, and Hederagenin. The molecular dynamics simulations and MM-PBSA analysis were implemented based on the docking results. The free binding energy of Veratramine, Azulene, Hupehenine, and Hederagenin was estimated. Besides the favourable binding point, the ligands also showed good hydrogen bonding and other interactions with key residues of the enzyme's active site. The natural compounds were also experimentally investigated for their effect on the *L. donovani* promastigotes and murine macrophage (J774A.1). A good antileishmanial activity by the compounds on the promastigotes was observed as estimated by the MTT assay. The *in-vitro* experiments revealed that Hupehenine (IC_{50} = 7.34 ± 0.37 μM) and Veratramine (12.46 ± 2.28 μM) exhibited better inhibition than Hederagenin (23.36 ± 0.54 μM) and Azulene (24.42 ± 3.28 μM). This work has positively demonstrated major inhibitors against the enzyme as potential anti-leishmanial compounds.

---

*Part of the work published in **I**nternational Journal of Biological Macromolecules**,** 2023, 232, 31, 123441

2.1 Introduction

Leishmaniasis is a parasitic disease widely spread in the tropics and subtropics areas of Asia, Africa, America and Europe. It is classified as a Neglected Tropical Disease (NTD) by the WHO. Among the global population worldwide, the *Leishmania*-infected population is approximately 10-12 million, and approximately 0.9-1.6 million new infected individuals are reported annually. Leishmaniasis is said to cause 20-50 thousand deaths annually. Country-wise distribution of the disease shows that India, Nepal, Bangladesh and Sudan contribute 90% of the total cases. In India, the dominant states affected by this disease are Uttar Pradesh, Bihar, Delhi, Jharkhand, West Bengal, Gujarat, Madhya Pradesh, and Kerala. Bihar contributes 40-50% of world leishmaniasis cases and 90% of total cases in India (Efstathiou and Smirlis, 2021; Samuel Singh, 2019). The main factor contributing to the vast spread of the disease is the diversity of the *Leishmania* species. More than 20 different species of *Leishmania* are responsible for the disease, including *L. amazonensis, L. major, L. mexicana, L. infantum, L. donovani, and L. tropica.* Among significant factors for the cause of the disease are lifestyle (socioeconomic), geographic location, and physical state of the individual (eg, immunocompromised individuals). Since the disease spreads mainly among underprivileged people, there is limited funding for developing drugs and treatment strategies. Hence, a robust and cost-effective drug development strategy is the need of the hour for more comprehensive therapeutic options to treat Leishmaniasis (Efstathiou & Smirlis, 2021; Samuel Singh, 2019).

Leishmaniasis is caused by an obligate digenetic protozoan parasite called *Leishmania,* where the bite of an infected sandfly spreads the disease. The parasite contains two developmental stages, the first promastigote stage present in the insect vector and the second amastigote stage present in the mammalian host. The extracellular promastigote form of the parasite enters the human host, multiplies in the phagolysosomes of macrophages and then transforms into an intracellular amastigote. The disease has three major classifications: cutaneous,

mucocutaneous, and visceral. Visceral leishmaniasis causes 30,000 new cases annually in over 83 countries. It is also considered to be the most lethal form and can be fatal. A person infected with visceral leishmaniasis has prolonged fever, hepatomegaly, splenomegaly, pancytopenia, anaemia, and weight loss (Chakravarty and Sundar, 2019b; Efstathiou and Smirlis, 2021; Samuel Singh, 2019). Current treatment options for leishmaniasis are not robust, have side effects (pentavalent antimonials, pentamidine), and are expensive (ambisome, paromomycin). Some medicines have also shown drug resistance (pentavalent antimonials, miltefosine) (Roatt *et al.*, 2020), hence it is important and clinically relevant to develop new drug targets which will assist in the generation of new molecules.

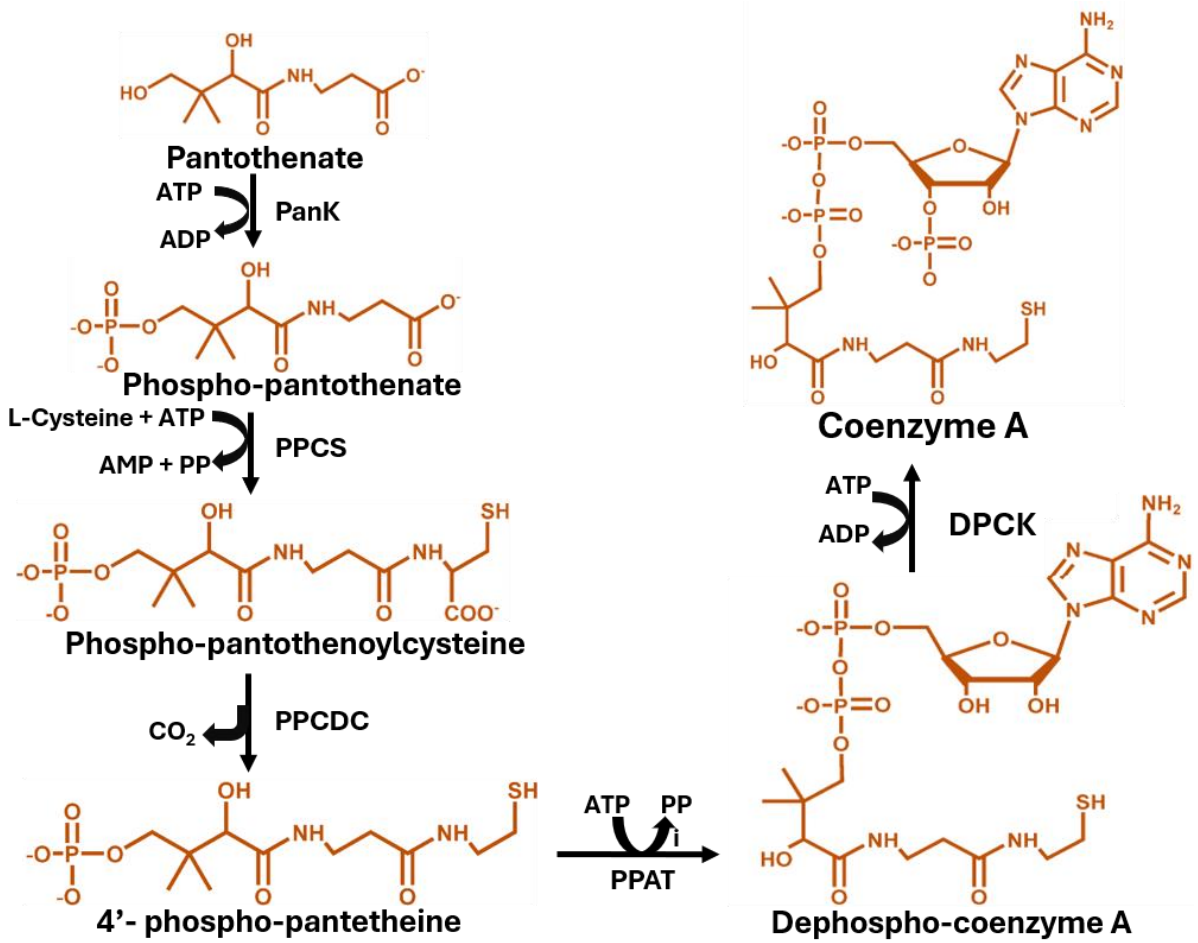

Figure 6: Enzymatic pathway of coenzyme A biosynthesis in *Leishmania*. The diagram illustrates the sequential enzymatic steps leading to the production of Coenzyme A.

A critical molecule which plays various roles in the survival of a cell is Coenzyme A. The synthesis of Coenzyme A consists of five significant steps in *Leishmania* in which Pantothenate is used as an initial substrate. The first step involves the conversion of Pantothenate to 4'-Phosphopantothenate by Pantothenate kinase (PanK). The second step produces 4'-Posphopantothenoylcysteine from 4'-Phosphopantothenate using Phosphopantothenoylcysteine synthetase (PPCS), converted to 4'-Phosphopantetheine catalysed by Phosphopantothenoylcysteine decarboxylase (PPCDC). The fourth step involves the conversion of 4'-Phosphopantetheine to Dephospho-coenzyme A, assisted by Phosphopantetheine adenylyltransferase (PPAT). The final stage of Coenzyme A production consists of the transformation of Dephospho-coenzyme A to Coenzyme A by Dephospho-coenzyme A kinase (DPCK) (Figure 6) (Efstathiou and Smirlis, 2021; Gudkova et al., 2012). Coenzyme A acts as a necessary cofactor for many enzymes and is a part of many biochemical processes, such as fatty acids, ketones, and cholesterol metabolism. It plays a vital role in the cell cycle, signal transduction, membrane trafficking and differentiation, which is crucial for the parasite's survival and host infection (Efstathiou and Smirlis, 2021; Gudkova et al., 2012). DPCK was used as a target for drug discovery because it is one of the rate-limiting steps in the Coenzyme A synthesis pathway(Shimosaka et al., 2019a). Ideally, the target chosen for drug discovery should be absent, or a different target form should be present in humans. Moreover, it is also important that such a drug target should be essential for the pathogen's survival. DPCK is considered a promising drug target as it is necessary to thrive the parasite, which ultimately causes leishmaniasis in humans. Also, in humans, the final step of Coenzyme A synthesis is completed using a bifunctional enzyme, Coenzyme A synthase, which performs the dual role of PPAT and DPCK. Hence, it suits as a drug target against *Leishmania donovani* to treat Leishmaniasis (Chawla and Madhubala, 2010).

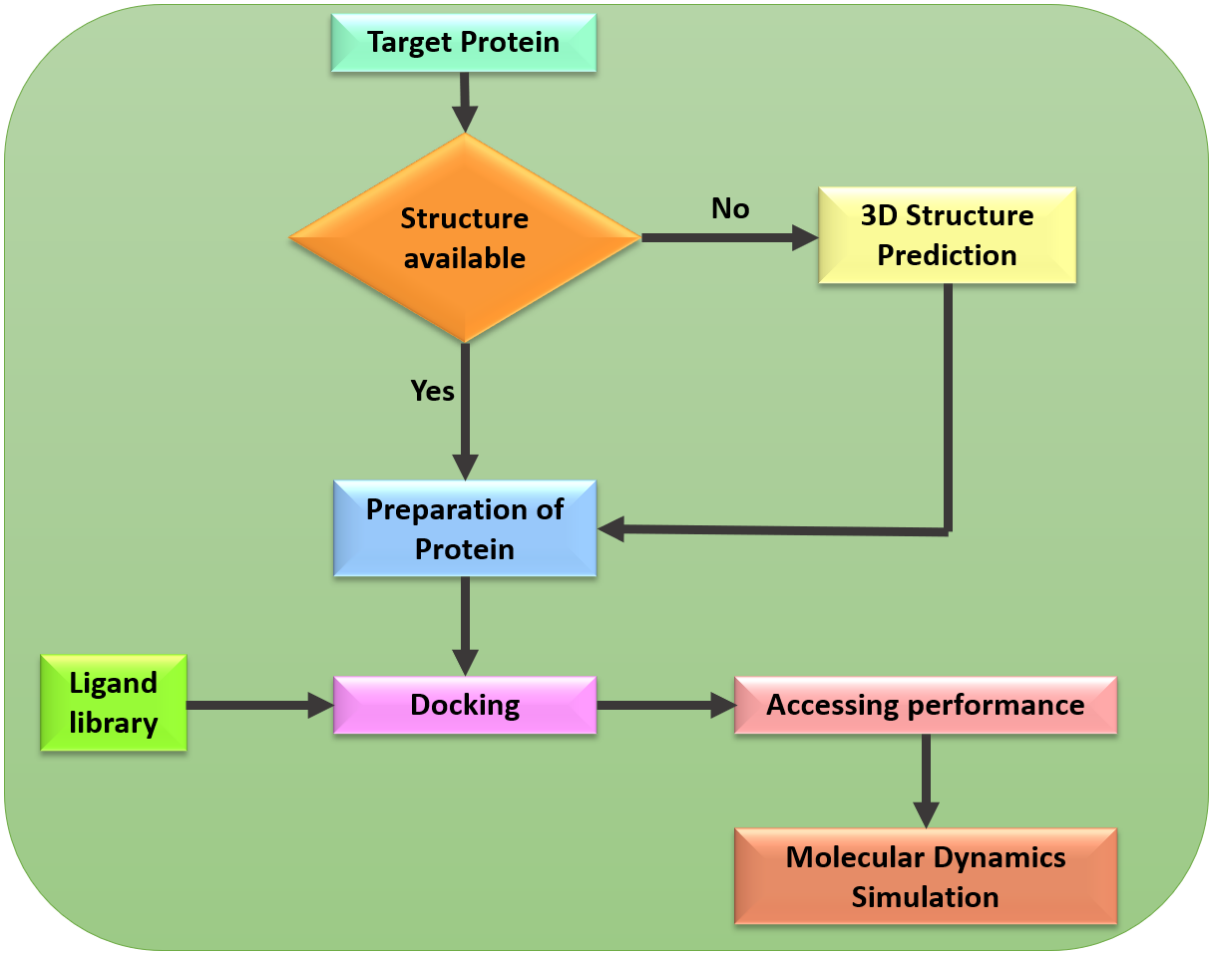

Figure 7: Workflow illustrating the approach to structure-based drug design.

Earlier studies have reported on exploiting the Coenzyme A biosynthesis pathway to find DPCK-specific inhibitors as a potential drug molecule. A. Nurkanto *et al.* have identified and validated drug molecules which have shown inhibitory effects against both the DPCK enzyme as well as on the *P. falciparum* parasite (Nurkanto et al., 2018b).

Here, the Computer-aided Drug Discovery (CDD) method was used, one of the most predominant contemporary methods for pre-clinical drug discovery. Several computational approaches and software combinations have yielded drugs now approved for clinical trials (Figure 8). The Structure-based Virtual Screening (SVS) approach was employed, also known as receptor-based virtual screening. This technique screens the known protein structures with a ligand database to get the desired drug candidate (Sabe et al., 2021). The docking and post-

docking examinations of the *Leishmania donovani* Dephospho-coenzyme A kinase (LdDPCK) was performed with the natural products datasets to get the best hit compounds.

2.2 Materials and methods

2.2.1 Preparation of target protein and ligands

The sequences of *Leishmania donovani* Dephospho-coenzyme A kinase (LdDPCK) and Human Dephospho-coenzyme A kinase (COASY) were obtained from the UniProt database (Bateman et al., 2021). Homology modelling was executed using the SWISS-MODEL server since their crystal structure were unavailable (Naik et al., 2020; Waterhouse et al., 2018). Considering the highest per cent identity according to BLAST, the crystal structures of Dephospho-coenzyme A kinase from *Burkholderia vietnamiensis* and Dephospho-coenzyme A kinase with adenosine-5'-diphosphate from *Escherichia coli* were selected as a template for designing LdDPCK and COASY models, respectively (Altschup et al., 1990). The models were submitted to GalaxyRefine for further refinement and conformational corrections (Ko et al., 2012). The final models were confirmed by Ramachandran Plot using the SWISS-MODEL server (Naik et al., 2020; Waterhouse et al., 2018). The active site residues were predicted using the COACH server (Yang et al., 2013) and then subjected the protein models (LdDPCK and COASY) to energy minimisation with the help of a Swiss PDB viewer (Ciucx and Peitsrh Urctrophuresis, 1997). In this study, the natural products from the ZINC Database were harnessed as ligands for virtual screening (Irwin and Shoichet, 2005). The SDF files of natural products from the database were converted to PDBQT files for docking using Open Babel (O'Boyle et al., 2011).

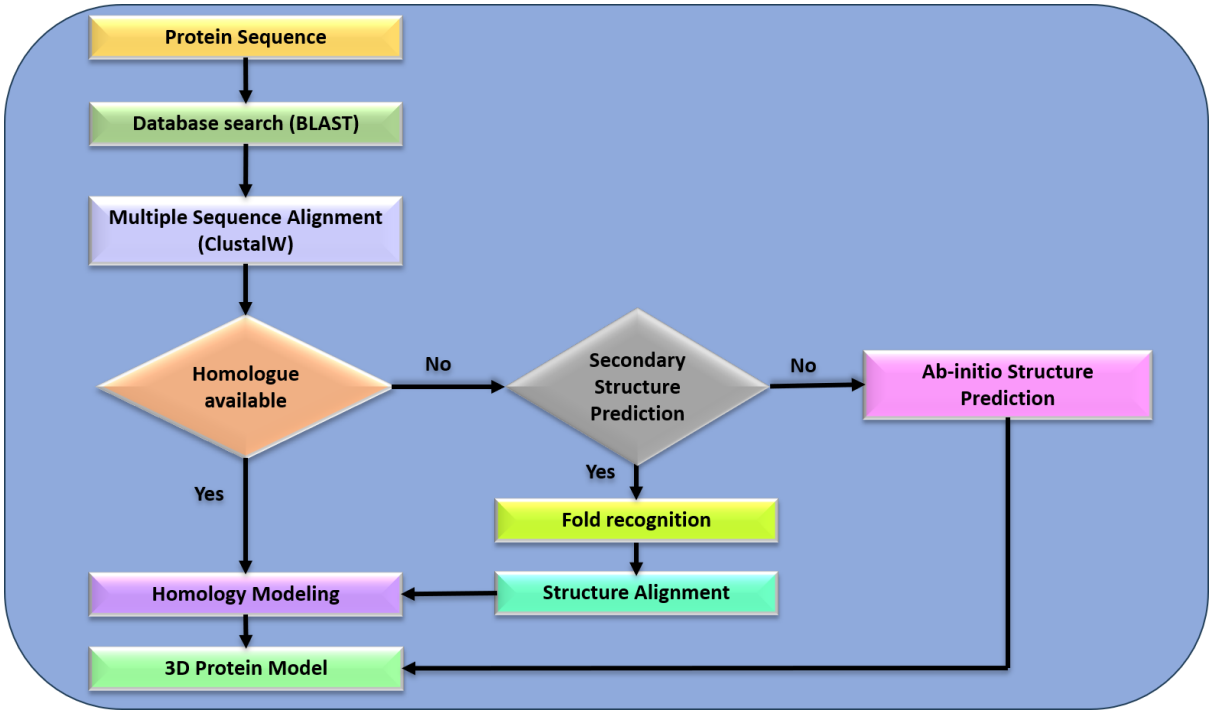

Figure 8: Computational workflow for protein structure prediction. A schematic representation of the computational approach employed to predict protein structures, illustrating the key steps from sequence input to final 3D structural modelling and validation.

2.2.2 Virtual screening and molecular docking study

For docking studies, the proteins were considered as rigid structures and the ligands as flexible structures. The GPFs (Grid Parameter Files) were generated and defined as 69.45, 65.354 and 56.439 for LdDPCK and 11.432, 11.764 and 5.669 for COASY as X-, Y- and Z- coordinates, respectively. The virtual screening of natural products was performed with the help of Racoon and AutoDockTools 1.5.6 for 100 conformations (Morris et al., 2009). The Lamarckian Genetic Algorithm and the AMBER force field were applied for docking(Goodsell et al., 1996; Kundu and Dubey, 2021). Eventually, lead natural compounds were selected based on the highest binding energy difference between LdDPCK and COASY. The 2-D ligand-protein interactions were visualised using Discovery Studio Client (Dassault Systèmes BIOVIA. Discovery studio visualiser, v.20.1.0.19295. San Diego: DassaultSystèmes. 2020., n.d.).

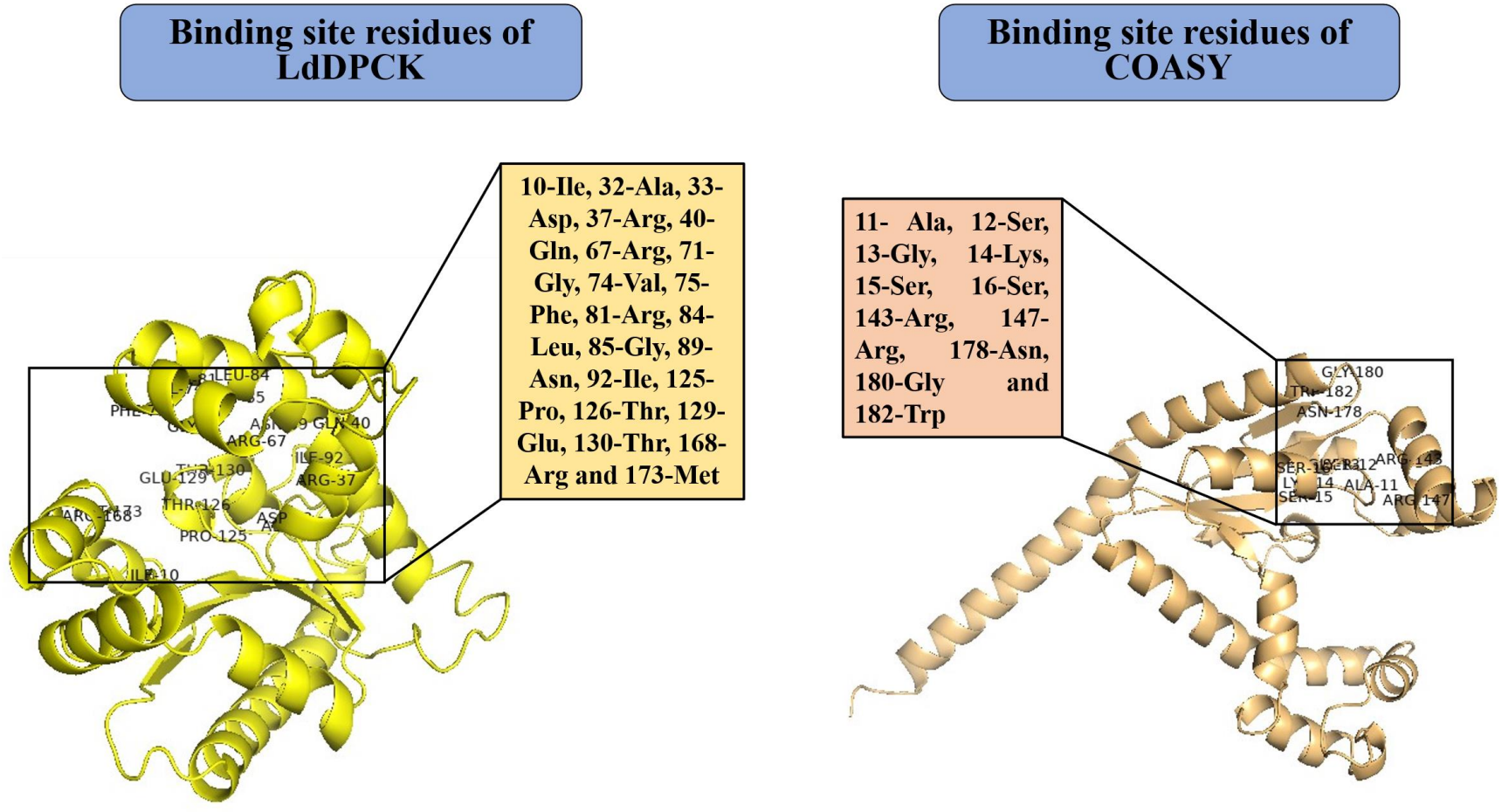

Figure 9: Structural comparison showing distinct binding site residues between *Leishmania donovani* DPCK and its human ortholog COASY.

2.2.3 ADME analysis

The pharmacokinetic properties of the top 25 natural compounds were analysed using the SwissADME server to evaluate adsorption, distribution, metabolism and excretion (ADME) and drug likeliness by Lipinski's rule of five (Daina et al., 2017).

2.2.4 MD Simulations study

The top four commercially available natural compounds were selected and subjected to MD Simulations to validate the docking results via GROMACS v 2018.8 (Hess et al., 2008). The final M D production run was employed for both apoprotein and protein-ligand complexes using the GROMOS 54a7 force field (Abraham et al., 2015). The system's initial conditions were defined as a 1.2 nm cube with SPC/E water molecules as a solvation system, and performed ionisation using Na^+ and Cl^- ions for charge neutralisation. The energy minimisation of all the systems was performed using the steepest descent algorithm with 50,000 as maximum steps and 1000 kJ/mol/nm tolerance. The parameter files and ligand topology files were generated using PRODRG server v. 2.5. After this step, equilibration of the system in two phases, NVT and NPT, with a constant number of particles, volume, temperature and pressure for 1 ns has been performed (Borkotoky and Banerjee, 2021; Bussi et al., 2007). The two-phase equilibration was performed using V-rescale and Parrinello-Rahman at 310 K and 1 bar (Borkotoky et al., 2021; Borkotoky and Banerjee, 2021). All bonds were constrained using Linear Constraint Solver (LINCS) (Hess et al., 1997). The MD simulations for both apoprotein and protein-ligand complex were executed for 130 ns, and the trajectories were analysed using the inbuilt GROMACS functions (Kundu and Dubey, 2021).

2.2.5 MM-PBSA free energy analysis

Post-MD simulations, the selected compounds were analysed for binding free energy using Molecular Mechanics Poisson-Boltzmann Surface Area (MM-PBSA) (Genheden and Ryde, 2015). The total free binding energy and the energy contribution by each residue were estimated with the GROMACS platform using the gmx_mmpbsa tool. The MM-PBSA method applies the following equation (equation 1) for calculating the Gibbs' free energy of binding.

$G_{bind} = (\Delta E_{elec} + \Delta E_{vdw}) + (\Delta G_{polar} + \Delta G_{SASA})$ …….. equation (1)

Where, G_{bind} is binding free energy, ΔE_{elec} is electrostatic energy change, ΔE_{vdw} is van der waals energy change, ΔG_{polar} is polar solvation energy change, and ΔG_{SASA} is non-polar solvation energy change. The nonpolar solvation energy was calculated using the SASA model (Borkotoky et al., 2021).

2.2.6 Cultures and chemicals

Leishmania donovani AG83 [MHOM/IN/1983/AG83] was grown at 25˚C in M199 media supplemented with fetal bovine serum (10%) and antibiotics (100 U/ml penicillin and 100µg/ml streptomycin). The J774A.1 cell line was grown at 37˚C and 5% CO_2 in RPMI 1640 media supplemented with fetal bovine serum (10%) and antibiotics (100U/ml penicillin and 100µg/ml streptomycin). All chemicals used for cell culture were of the highest grade procured from Sigma-Aldrich and Merck.

2.2.7 Effect of selected LdDPCK inhibitors on *L. donovani* proliferation

The effect of LdDPCK inhibition on the growth of *L. donovani* promastigote cells was evaluated using an MTT assay, a colorimetric assessment of cell proliferation. MTT [3-(4,5-dimethylthiazol-2-yl)-2,5-diphenyltetrazolium bromide] is a yellow-coloured compound which is reduced to formazan (a purple-coloured product) by the mitochondrial enzymes of the

viable cells. The test compounds (dissolved in DMSO) were serially diluted in M199 media in a 96-well plate with a total volume of 200 µl. The wells preloaded with different concentrations of compounds were seeded with *L. donovani* promastigote cells (2.5×10^6 cells/ml) grown in M199 media. Culture without drug treatment was used as a negative control, M199 media was taken as a blank, and the Miltefosine concentration, which showed complete inhibition, was used as a positive control. The cultures were incubated for 48 hours in the dark at 25˚C. The MTT reagent (0.5 mg/ml) was added to the cultures and incubated for 4 hours in the dark at 25˚C. After incubation, the plates were centrifuged at 4000 rpm for 45 min. The pellets (formazan crystals) were dissolved in DMSO, and the absorbance was measured using a microtiter plate reader (BioTek Synergy HT) at 570 nm. The IC_{50} values of each compound were calculated by plotting the percentage of cell viability versus the concentration of the compound (Baranwal et al., 2018; Bhalla et al., 2018; Saudagar and Dubey, 2011).

2.2.8 Cytotoxic effect of LdDPCK inhibitors on J774A.1 cell line

The J774A.1 cell line, grown in RPMI 1640 media, was used to determine the CC50 of the natural compounds using an MTT assay. J774A.1 cells (5×10^4 cells /ml) were seeded into a 96-well plate and allowed to adhere overnight at 37˚C and 5% CO_2. After incubation, the media was discarded from the wells to remove the nonadherent cells. The test compounds, serially diluted in RPMI 1640 media, were added to the overnight-grown culture in a total volume of 200µl and incubated for 48 hours at 37˚C and 5% CO_2. The cell culture without any drug was considered a negative control, and the RPMI 1640 media was taken as a blank. After 48 hours of treatment, the wells were incubated with an MTT reagent (0.5 mg/ml) for 4 hours at 37˚C and 5% CO_2. The media was removed and the crystals were dissolved in DMSO. The absorbance was measured at 570 nm using a microtiter reader plate (BioTek Synergy HT). The

percentage cell viability versus concentration of compound plot was used to calculate the CC_{50} of the selected compounds (Mendes et al., 2022a; Saudagar and Dubey, 2014a).

The selectivity index (SI), expressed as the ratio between cytotoxicity in the J774A.1 cell line (CC_{50}) and the inhibition of *L. donovani* activity (IC_{50}) was estimated for each compound (SI = CC_{50} / IC_{50}) (Mendes et al., 2022b).

2.2.9 Statistical analysis

All the experiments were carried out in triplicate, and at least two independent experiments were performed for each analysis. The IC_{50} and CC_{50} results were expressed as the mean ± standard deviation of two independent experiments.

2.3 Results

2.3.1 Protein model

The structure of *Leishmania donovani* Dephospho-coenzyme A kinase (LdDPCK) and Human Dephospho-coenzyme A kinase (COASY) was generated by the homology modelling method. The templates used for constructing the models showed greater than 30% identity with the original query sequence, estimated by the Basic Local Alignment Search Tool (BLAST) (Figure 7). The LdDPCK model exhibited 96.89%, and the COASY model demonstrated 97.82% Ramachandran favoured regions, which can be considered as a precise model (Figure 10). The active binding site of LdDPCK was predicted through the COACH server (Yang et al., 2013), which incorporates the following residues: 10-Ile, 32-Ala, 33-Asp, 37-Arg, 40-Gln, 67-Arg, 71-Gly, 74-Val, 75-Phe, 81-Arg, 84-Leu, 85-Gly, 89-Asn, 92-Ile, 125-Pro, 126-Thr, 129-Glu, 130-Thr, 168-Arg and 173-Met (Figure 9).

2.3.2 Molecular docking analysis

In this study, around 48,164 natural products were subjected to *in-silico* molecular docking with LdDPCK and COASY using AutoDockTools. The docking score of LdDPCK with the ligand dataset ranges from -11 kcal/mol to -2.7 kcal/mol. Virtual screening was done based on the highest binding energy differences between the two proteins. The drug shows more binding affinity towards LdDPCK than COASY, which is one of the fundamental ideas in the drug discovery process. The top 10 natural products were sorted and computed to evaluate ADME and Lipinski's rule of five, considering parameters such as molecular weight, Lipinski's violation, Log S, Log P, and TPSA for screening the natural compounds. Finally, the top four commercially available natural compounds were adopted for further analysis. These compounds were Veratramine (ZINC000003875407), Azulene (ZINC000001570209), Hupehenine (ZINC000100038283) and Hederagenin (ZINC000004166079) (Table 6). All the natural compounds exhibited good binding affinity towards LdDPCK. The binding energies of Veratramine, Azulene, Hupehenine and Hederagenin were computed to be -10.14 kcal/mol, -6.78 kcal/mol, -10.47 kcal/mol, and -10.55 kcal/mol, respectively. As calculated by AutoDockTools, Hederagenin had the least Ki (Inhibition constant) value (18.57 nM), followed by Hupehenine (21.31 nM), Veratramine (36.73 nM) and Azulene (10.64 μM) (Table 5). The compound Veratramine formed three hydrogen bonds with the binding site residues Ala-11, Ser-15, and Arg-81; however, Azulene did not form any hydrogen bonds with the residues. The compounds Hupehenine and Hederagenin formed a single hydrogen bond with Thr-126 and Gly-71 residues, respectively (Table 8). The 3-D interactions of the natural products with the protein's active site residues were visualised through Discovery Studio Client in Figure 11.

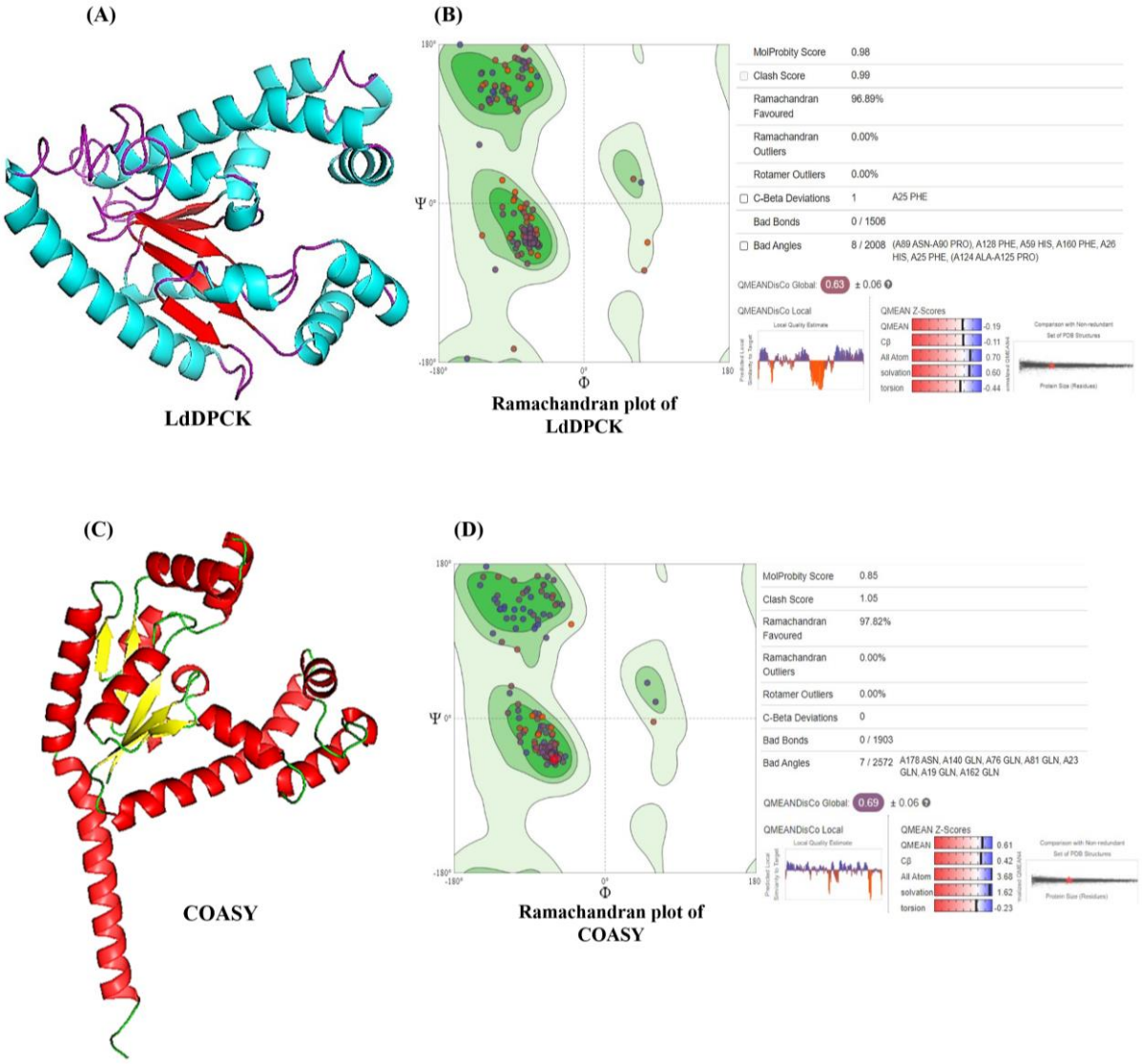

Figure 10: (A) Computationally predicted three-dimensional structure of *Leishmania donovani* dephospho-coenzyme A kinase (LdDPCK), generated using homology modelling approaches, (B) Assessment of the structural integrity and stereochemical quality of the LdDPCK model through Ramachandran plot analysis, indicating the distribution of backbone dihedral angles (ϕ and ψ), (C) In silico-predicted tertiary structure of human Coenzyme A synthase (COASY), modelled using a similar computational pipeline for structural comparison with the parasite homolog, and (D) Validation of the predicted COASY structure via Ramachandran plot analysis, confirming the reliability of the model based on conformational angle distributions.

Table 5: Binding affinities of selected natural compounds against LdDPCK and human COASY, obtained through molecular docking studies.

ZINC database ID	Molecular Formula	Chemical Structure	LdDPCK Binding affinity (kcal/mol)	COASY Binding affinity (kcal/mol)	Difference in Binding affinity (kcal/mol)
ZINC000042887783	C30H48O4	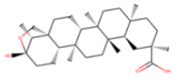	-12.12	-8.47	3.65
ZINC000056871311	C30H49N3O2	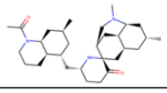	-12.19	-8.73	3.46
ZINC000003875407.	**C27H39NO2**	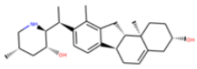	**-10.14**	**-7.00**	**3.14**
ZINC000005762506	C30H50O2	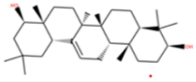	-10.81	-7.96	2.85
ZINC000253505669	C36H46O	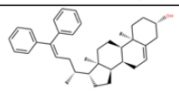	-10.56	-7.81	2.75
ZINC000001570209.	**C10H8**	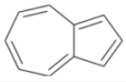	**-6.78**	**-4.03**	**2.75**
ZINC000100038283.	**C27H45NO2**	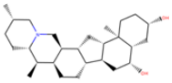	**-10.47**	**-7.80**	**2.67**
ZINC000004166079.	**C30H48O4**	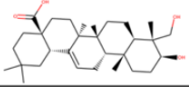	**-10.55**	**-7.91**	**2.64**
ZINC000118913881	C29H50O	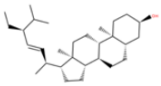	-9.45	-6.90	2.55
ZINC000003847555	C30H48O3	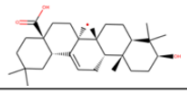	-10.62	-8.09	2.53

Table 6: ADME analysis of natural compounds in complex with LdDPCK.

Compounds	**MW (Da)**	**H - Acceptor**	**H - Donor**	**TPSA (Å^2)**	**LogP**	**LogS**	**Lipinski violations**
Veratramine	409.6	3	3	52.49	4.33	-5.13	1
Azulene	128.17	0	0	0	3.04	-3.39	0
Hupehenine	415.65	3	2	43.7	4.25	-5.91	1
Hederagenin	472.7	4	3	77.76	5.37	-6.94	1

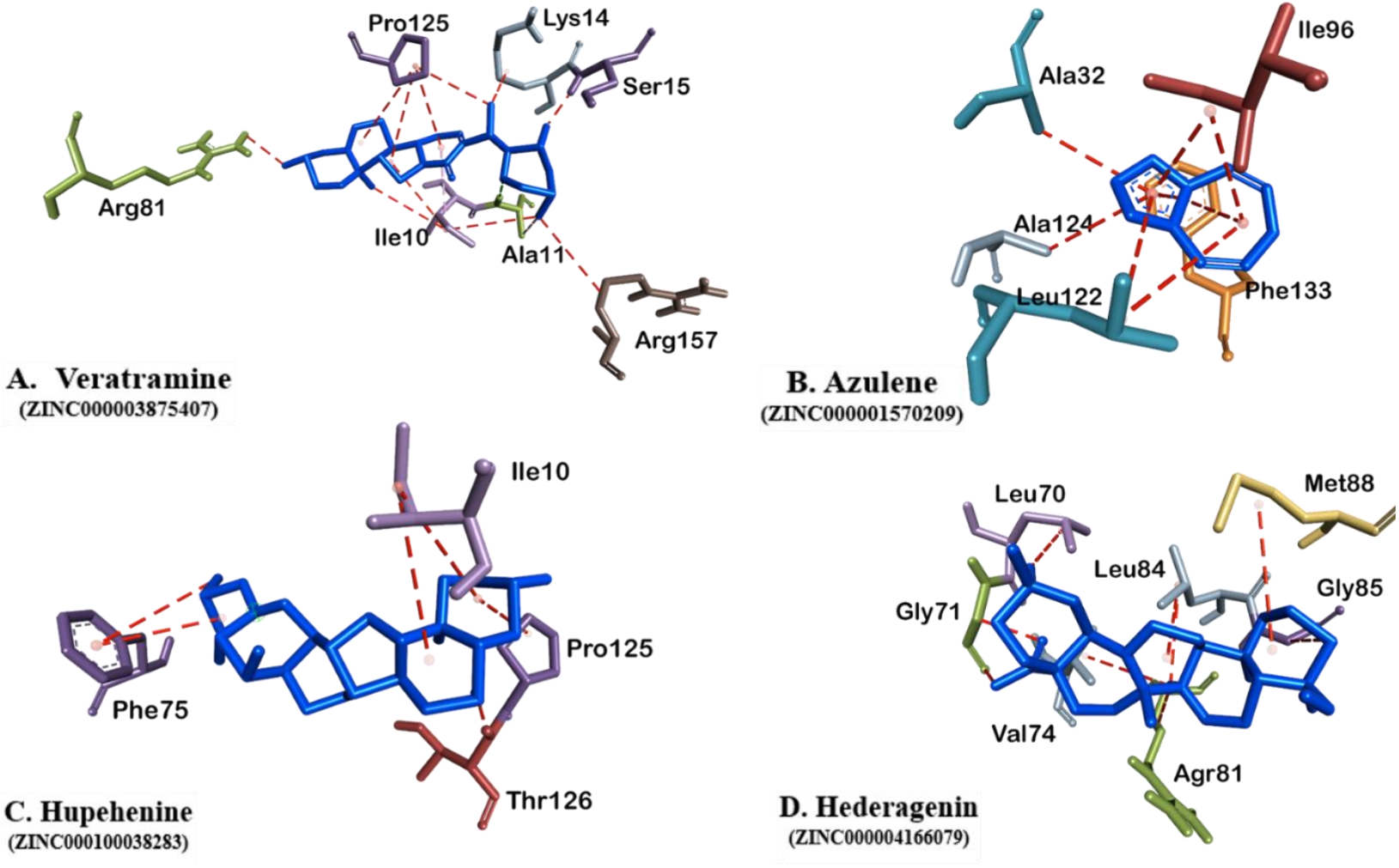

Figure 11: 3-D interactions of LdDPCK with natural compounds depicting hydrogen bonds and other non-covalent bonds, **(A)** Veratramine, **(B)** Azulene, **(C)** Hupehenine and **(D)** Hederagenin.

2.3.3 Molecular dynamic simulation (MD Simulations) analysis

After performing molecular docking and virtual screening, the hit compounds were analysed by conducting MD Simulations for 130 ns. After completing MD simulations, the root-mean-square deviation (RMSD) analysis of the apoprotein and the ligand-protein complexes was executed. The results showed that the complex structures were comparatively more stable than the LdDPCK protein alone. The RMSD of the apoprotein was observed to be constantly deviating throughout the simulation and reached a maximum of ~ 0.8 nm at the end of the simulation (Figure 13). It was observed that the protein-drug complexes expressed deviation during the initial time of the run, that is, up to 10 ns, and then consecutively attained stability after this time. All the complex systems exhibited RMSD values between ~ 0.3 nm and 0.5 nm at the end of the run. This is lower compared to the apoprotein, eventually making the system stable. It is interesting to note that the Hederagenin system represents the slightest deviation throughout the simulation, followed by Azulene. Although Veratramine and Hupehenine systems showed minor variations, they were comparatively stable throughout the simulation process.

The RMSF data of the active site residues were plotted to examine the conformational fluctuations occurring at the active site of the LdDPCK protein in the presence of the ligands for the 130 ns simulation time. It was observed that the RMSF values of the LdDPCK protein complex with Hupehenine, Hederagenin, and Veratramine did not exceed an average of 0.2 nm, owing to fewer fluctuations and more conformational stability (Figure 13). However, in the presence of Azulene, the RMSF values represented a maximum fluctuation of ~0.65 nm. The Azulene system appeared to fluctuate more at the residues 33-Asp, 37-Arg, 67-Arg, 71-Gly, 74-Val, 75-Phe, and 81-Arg.

The radius of gyration (Rg) and SASA data indicate the compactness of the protein structure over time and, therefore, are measures of the protein folding in the presence of the ligands. Lower values indicate more compactness or less unfolding of the protein and vice versa. A remarkable increase in compactness (folding) of the protein and the complexes was encountered at around 110 ns. The Rg values were least for the Hederagenin complex system, followed by Hupehenine and Veratramine, indicating that the protein folding was more in the presence of these three compounds. The Rg trajectory of the Azulene complex showed higher values until ~ 90 ns and then declined significantly (Figure 14). The SASA data showed a similar fashion of trajectory as Rg data, while the SASA values decreased from ~160 nm^2 to ~145 nm^2 at the end of the simulation. Fewer residues of the Hederagenin complex were exposed to the solvent in the system owing to a more compact structure (Figure 14). The residues of the system exposed to the surface and available for solvent interaction in increasing order were: Hederagenin, Hupehenine, Veratramine, Azulene, and Apoprotein.

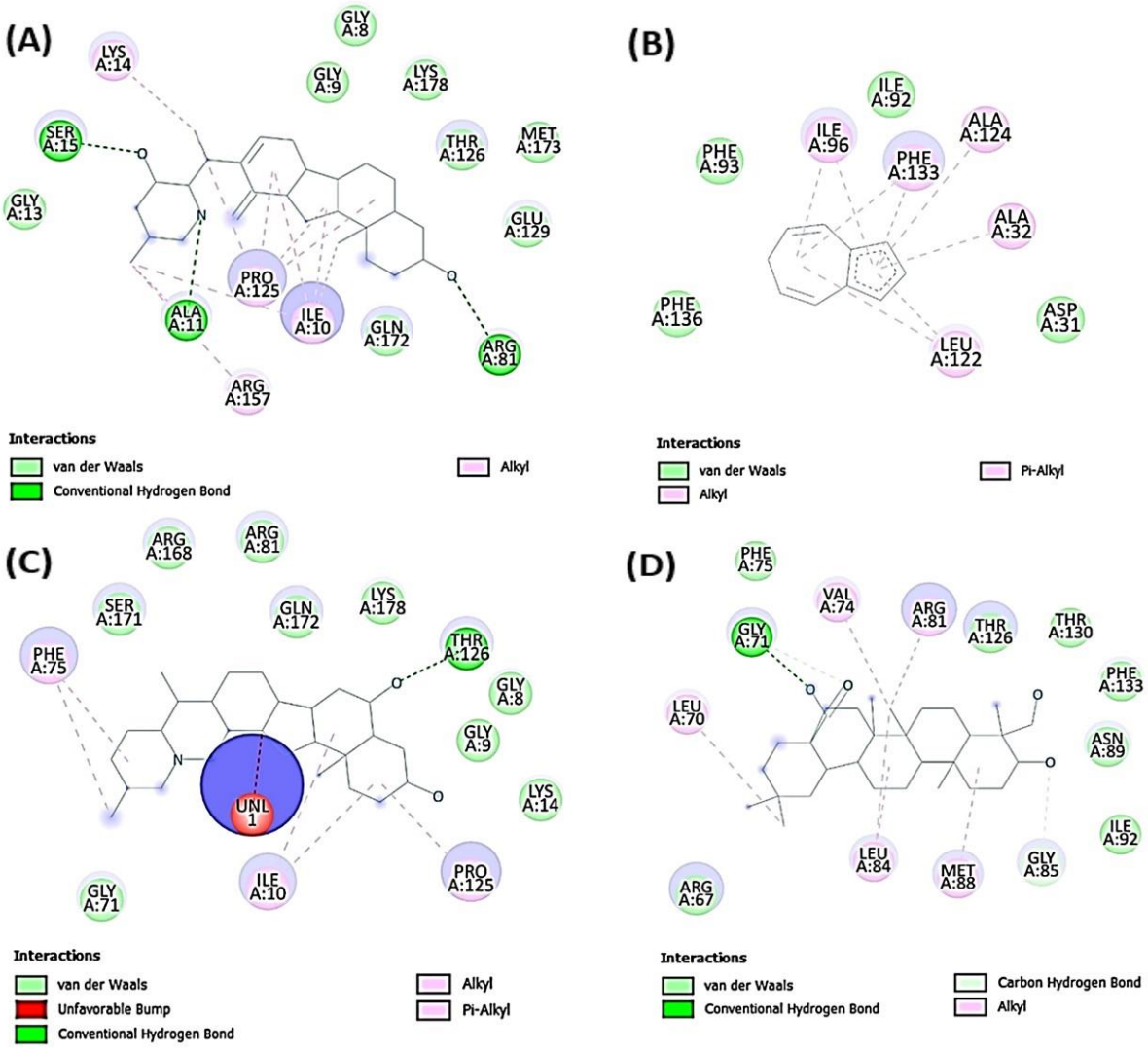

Figure 12: 2-D interactions of LdDPCK with natural compounds depicting hydrogen bonds and other non-covalent bonds, **(A)** Veratramine, **(B)** Azulene, **(C)** Hupehenine and **(D)** Hederagenin.

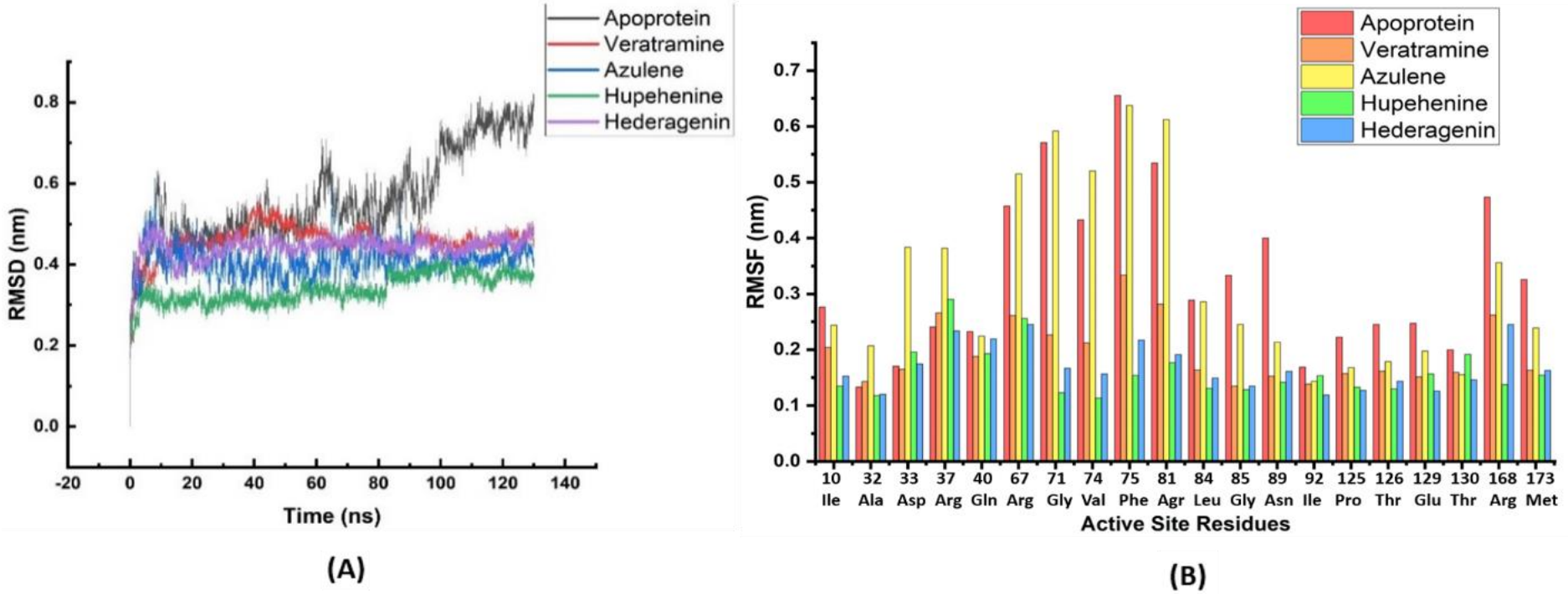

Figure 13: Comparative analysis of MD simulation results of apoprotein and protein-ligand complex with Veratramine, Azulene, Hupehenine and Hederagenin, calculated over 130ns. **(A)** Analysis of the backbone RMSD trajectories and **(B)** Analysis of RMSF trajectories of substrate binding site residues.

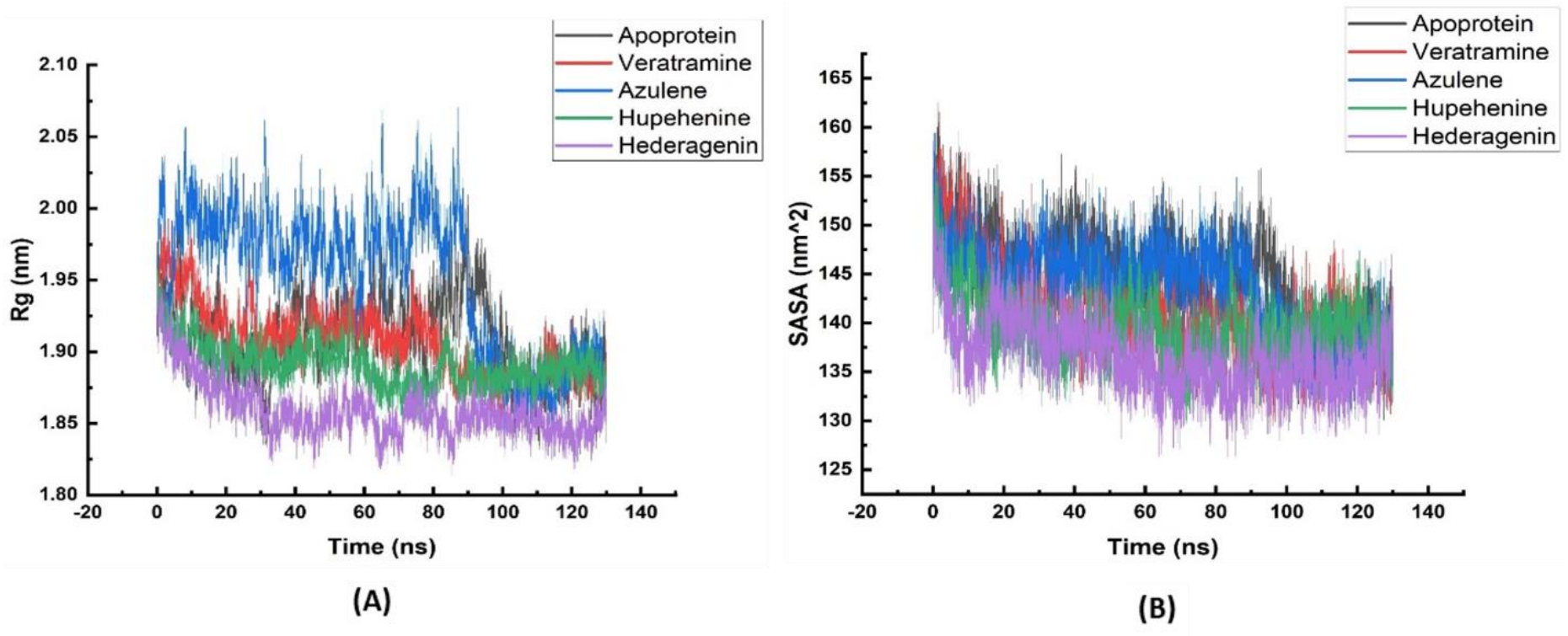

Figure 14: Analysis of MD simulation results and comparison of apoprotein with Veratramine, Azulene, Hupehenine and Hederagenin complexes. **(A)** Graph of Radius of gyration (Rg) analysis and **(B)** Graph of SASA analysis.

2.3.4 MM-PBSA analysis

To inspect the protein-ligand complexes in terms of energy components, the free binding energy of the system was estimated using MM-PBSA. The energy contributed individually by Van der Waals, Electrostatic and Polar solvation was calculated for each system. The detailed results are indicated in Table 7. The LdDPCK complex with Hederagenin possesses the highest binding energy of -160.345 ± 20.605 KJ/mol, followed by Azulene, Hupehenine and Veratramine complexes, which exhibited a binding energy of -80.144 ± 8.776 KJ/mol, -53.233 ± 65.247 KJ/mol and -33.673 ± 58.542 KJ/mol, respectively (Table 7).

Table 7: MM/PBSA free energy analysis of selected natural compounds.

Compounds	Van Der Waals (KJ/mol)	Electrostatic (KJ/mol)	Polar solvation (KJ/mol)	Binding Energy (KJ/mol)
Veratramine	-45.257 ± 67.821	-0.980 ± 3.358	17.258 ± 31.432	-33.673 ±58.542
Azulene	-83.590 ± 7.814	0.146 ± 0.848	11.926 ± 5.090	-80.144 ± 8.776
Hupehenine	-63.806 ± 71.133	0.570 ± 2.430	17.681 ± 35.894	-53.233 ± 65.247
Hederagenin	-195.164 ± 18.660	0.832 ± 3.327	53.269 ± 15.649	-160.345 ± 20.605

2.3.5 Hydrogen Bond Analysis

For further analysis of the current simulation results, ligands' potential hydrogen bonding patterns with the active site of the enzyme were estimated. The results indicate that Veratramine and Hupehenine form approximately one hydrogen bond on average, whereas hederagenin forms two hydrogen bonds with various active site residues. Arg67, Val74, Phe75, Arg168, Thr126, Glu129, Thr130, Gly85, and Asn89 are some critical active site residues that are heavily involved in protein-ligand interaction (Table 8). The hydrogen bonding and other non-

covalent interactions with similar residues were reported during the molecular docking analyses.

Table 8: List of selected natural compounds with their respective binding energy, Ki and interactions with protein residues produced by *in-silico* docking.

Natural compounds	Binding affinity with LdDPCK (kcal/mol)	Ki	Residues forming	
			Hydrogen bond	Other interactions
Veratramine	-10.14	36.73 nM	Ala-11, Ser-15 and Arg-81	Gly-8, Gly-9, Ile-10, Gly-13, Lys-14, Pro-125, Thr-126, Glu-129, Arg-157, Gln-172, Met-173 and Lys-178
Azulene	-6.78	10.64 µM	-	Asp-31, Ala-32, Ile-92, Phe-93, Ile-96, Leu-122, Ala-124, Phe-133 and Phe-136
Hupehenine	-10.47	21.31 nM	Thr-126	Gly-8, Gly-9, Ile-10, Lys-14, Gly-71, Phe-75, Arg-81, Pro-125, Arg-168, Ser-171, Gln-172 and Lys-178
Hederagenin	-10.55	18.57 nM	Gly-71	Arg-67, Leu-70, Val-74, Phe-75, Arg-81, Leu-84, Gly-85, Met-88, Asn-89, Ile-92, Thr-126, Thr-130 and Phe-133

2.3.6 Cytotoxicity Analysis of LdDPCK inhibitors on *L. donovani* promastigotes and J774A.1 cell line

In order to validate the above-discussed results, in the next step, Hederagenin, Azulene, Hupehenine and Veratramine were tested in in vitro models using an MTT assay. A dose-response effect of the compounds on *L. donovani* promastigotes as well as in J774A.1 cell line was observed. The IC_{50} and CC_{50} were estimated by plotting percentage cell viability versus concentration of the natural compounds. A significant decrease in the viability of the parasite was observed above 6.25 µM concentration of Hupehenine, Azulene, and Veratramine, whereas for Hederagenin, it was found to be 12.5 µM. The IC_{50} values were 23.36 ± 0.54 µM for Hederagenin, 24.42 ± 3.28 µM for Azulene, 7.34 ± 0.37 µM for Hupehenine and 12.46 ± 2.28 µM for Veratramine (Table 9). Culture without drug treatment was used as a negative control, and the miltefosine concentration, which showed complete inhibition, was used as a positive control for promastigotes. The inhibition values were normalised against the positive control values, and the graph was plotted with untreated cultures as a negative control. A mammalian (murine) macrophage cell line, J774A.1, was used to analyse the effect of the selected natural compounds on host cells. The compounds exhibited varied half-maximal cytotoxic concentration (CC_{50}) ranging between 33.28 ± 2.39 µM (Hupehenine) and 21.91 ± 0.14 µM (Veratramine). Azulene and Hederagenin indicated a CC_{50} of 26.42 ± 0.0 µM and 24.21 ± 0.3 µM, respectively. The Selectivity index (SI) identifies the efficacy and safety of the compound and is defined as the ratio between CC_{50} and IC_{50}. As indicated in Table 9, only Hupehenine and Veratramine showed significantly high SI values of 4.5 and 1.7, respectively, while Azulene and Hederagenin indicated an unacceptable SI value (~ 1).

Table 9: IC_{50}, CC_{50} and SI of the natural compounds against promastigotes of *Leishmania donovani* and J774 cell lines after 48 hours of incubation.

Natural Compounds	IC_{50} of *L. donovani* (IC_{50} ± SD (µM))	CC_{50} of J774 (CC_{50} ± SD (µM))	SI (CC_{50} / IC_{50})
Veratramine	12.46 ± 2.28	21.91 ± 0.14	1.7
Azulene	24.42 ± 3.28	26.42 ± 0.0	1.0
Hupehenine	7.34 ± 0.37	33.28 ± 2.39	4.5
Hederagenin	23.36 ± 0.54	24.21 ± 0.3	1.0

2.4 Discussion

For decades, only the selected chemicals were administered to people affected by leishmaniasis: antimonials, amphotericin, paromomycin, and miltefosine. The existing chemotherapy is not satisfactory, and the combination therapy recently adapted to treat leishmaniasis is observed to be effective but causes relapse within a short period of administration. Hence, there is a continuous demand for new and efficient drug development for leishmaniasis, which requires more diverse research (Singh et al., 2014). Drug repurposing is a widely accepted and practical approach for neglected diseases as it requires the least time and resources to reach the affected people and makes the treatment economical. The strategy discussed in the present study increases the implementation of existing drugs for a different target, eliminating the initial steps of drug development and making the process rapidly advance towards execution (Pushpakom et al., 2018). A recent literature review suggests new strategies for treating leishmaniasis, including immunomodulators, nanotechnology-based drug delivery systems, and drug repurposing however these approaches are still under pre-clinical evaluation (Baranwal et al., 2018; Roatt et al., 2020).

Natural metabolites and their derivatives are a well-known source of biologically active compounds effective against many diseases, including leishmaniasis. Various natural compounds belonging to different families of chemicals have been reported to date and provide us with an opportunity to find a drug of interest. This primarily includes alkaloids, lignoids, saponins, lactones, quinones, and flavonoids (Cortes et al., 2020). Studies have shown that flavonoids and alkaloids are widely evaluated for their anti-parasitic properties. Triterpenoids, a subclass of alkaloids, have induced apoptosis and autophagy in *Leishmania sp* (Moulisha et al., 2010). Under the class of terpenes, sesquiterpenes have also shown anti-leishmanial action by depolarising the mitochondrial membrane and causing cell cycle arrest in the G0/G1 phase, leading to cell death by apoptosis (Cortes et al., 2020; Polonio and Efferth, 2008; Tiwari et al., 2017). Two flavonoids, luteolin and quercetin, were extensively evaluated and appear to act on the parasite by (i) cell cycle arrest in the G0/G1 phase leading to cell death by apoptosis and (ii) topoisomerase I inhibition. Patil *et al*. indicated that saponins possess anti-leishmanial activity, α-hederin, β-hederin, and hederagenin were effective against promastigote and amastigote forms. Being amphipathic, saponins act as a surfactant, hence it is anticipated to work on the parasite membrane, leading to a decrease in membrane potential (Polonio and Efferth, 2008; Salem and Werbovetz, 2006). Another natural compound, plumbagin, is a naphthoquinone which leads to topoisomerase II-mediated DNA cleavage and inhibits parasite proliferation (Polonio and Efferth, 2008).

The *in-silico* techniques were adapted to screen the natural product database. Docking and energy analysis have led us to the natural products, namely, Veratramine, Azulene, Hupehenine and Hederagenin, as the most potent compounds for possible inhibition of the LdDPCK enzyme. Three of these compounds are classified as alkaloids. Veratramine, an alkaloid, is isolated from rhizomes of *Veratrum* and is reported to be used to treat tumours by inhibiting its signal transduction (Wang et al., 2008). Hupehenine is an isosteroidal alkaloid isolated mostly

from *Bulbus fritillariae*, which is reported to possess antitussive effects (Wu et al., 2018). A pentacyclic triterpenoid saponin, hederagenin, is extracted from the *Hedera helix* and has numerous therapeutic effects, such as anti-inflammation, anti-depressant, liver protection, anti-aggregation of platelets, and hyperlipidemia therapy (Lu et al., 2015). Hederagenin has been reported to have an antileishmanial effect on *Leishmania donovani* promastigotes with an IC_{50} of 9.12 ± 0.29 µg/ml (Nkwenti Wonkam et al., 2020). Majester-Savornin *et al*. also indicated the inhibitory effect of hederagenin on *L. infantum* and *L. tropica* (Majester-Savornin et al., 1991), while an IC_{50} of 61.6 ± 0.25 µM has been recorded for intracellular *L. infantum* amastigotes (Rodríguez-Hernández et al., 2016). Azulenes are an isomer of naphthalene, also chemically known as cyclopentacycloheptene and are distilled from camomile oil (Leino et al., 2018). Azulene has appeared to treat HIV (Peet et al., 2016) and is also reported to have antileishmanial activity against *L. amazonensis* (Keshav et al., 2021).

As indicated, it is evident that these natural products, viz. Veratramine, Azulene, Hupehenine and Hederagenin have countless therapeutic values. Additionally, the cell proliferation test by using the MTT assay revealed a significant decrease in the viable cells corresponding to increasing concentrations of the tested compounds. Hupehenine (IC_{50} = 7.34 ± 0.37 µM) showed the best inhibition, followed by Veratramine (IC_{50} = 12.46 ± 2.28 µM). It was observed that Azulene (IC_{50} = 24.42 ± 3.28 µM) and Hederagenin (IC_{50} = 23.36 ± 0.54 µM) showed similar inhibition on promastigotes. However, the classical dose-dependent response may not be manifested by the tested compounds, as the IC_{50} values were calculated with an asymptote at 0% acquired by treatment with a miltefosine concentration at which complete inhibition of the proliferation of promastigotes was observed. The CC_{50} values for the J774A.1 cell line was observed to be the best for Hupehenine (CC_{50} = 33.28 ± 2.39 µM) and Veratramine (CC_{50} = 21.91 ± 0.14 µM). And also, the SI values of Hupehenine (SI = 4.5) and Veratramine (SI = 1.7) were comparatively higher than Azulene (CC_{50} = 26.42 ± 0.0 µM and SI = 1.0) and

Hederagenin (CC_{50} = 24.21 ± 0.3 µM and SI = 1.0). This indicates that Azulene and Hederagenin are equally toxic to J774A.1 cells and promastigotes. Although the individual effect of Azulene and Hederagenin on J774A.1 macrophage is not acceptable, but a safer and much lower concentration of these compounds can be used in synergy with other compounds to give the best results to inhibit *Leishmania donovani*. The *in-silico* studies were effectively executed and also validated the system in *in-vitro* models. The data deducted from the study have to be further validated by *in-vivo analysis, as the effect of these compounds could differ in the in-vivo* model from the parasites and mammalian cell line cultured in media.

2.5 Conclusion

This study attempts to find an effective cure for leishmaniasis using CDD. The current treatment methods given to patients with leishmaniasis have many disadvantages, such as being expensive, showing resistance, and being toxic in the long run. The SVS method was adopted to inhibit Dephospho-coenzyme A-kinase to overcome these drawbacks. Inhibition of Dephospho-coenzyme A-kinase activity ceases the synthesis of Coenzyme A, which suggests *Leishmania* cell death. The Natural products from the ZINC database were assessed for virtual screening. The hit compounds were selected after molecular docking and ADME analysis. The top four commercially available natural compounds were sorted, namely Veratramine (ZINC000003875407), Azulene (ZINC000001570209), Hupehenine (ZINC000100038283) and Hederagenin (ZINC000004166079). MD Simulations and the MM-PBSA study additionally confirmed the docking data. The RMSD, RMSF, Rg and SASA analyses show hederagenin as the best compound, followed by Hupehenine, Veratramine, and Azulene. The energy analysis and other parameters mentioned above suggest that these ligands can be significantly considered suitable anti-leishmanial compounds. The computational data is

additionally supported by the experimental data. The MTT assay was performed, and a proportional parasite death was observed with increasing concentrations of compounds. The IC_{50} values indicate that Hupehenine is the best inhibitor of *L. donovani,* followed by Veratramine, Hederagenin, and Azulene. Based on CC_{50} and SI values, Hederagenin and Azulene have been shown to be harmful to J774A.1 cells, but they can show better antileishmanial activity in combination with other compounds. Further *in-vivo* investigations have to be performed to get a deeper knowledge of the use of the above natural compounds as a drug against leishmaniasis.